negative spin density at the bound proton is thus evident.

Proton NMR spectra of the hydroxoiron(II) tetraarylporphyrin complexes differ from those previously reported for high-spin iron(II) derivatives in that the pyrrole proton signal at 32.8 ppm is shifted less downfield. The pyrrole chemical shift values range from approximately 50 to 60 ppm (25 °C, $(CH_3)_4Si$ reference) for respective 2-methylimidazole[18,19] and alkylmercaptide[17] complexes. The upfield bias for the signal in the hydroxide complex seemingly does not reflect a large upfield dipolar shift contribution, as the phenyl signals show only small shifts from the diamagnetic values. Upfield chemical shift contribution from a diamagnetic state in chemical or magnetic equilibrium with the high-spin state is ruled out by both the magnetic susceptibility determination and approximate NMR Curie law behavior. As was the case for hydroxoiron(II) octaalkylporphyrins, the importance of a π-spin delocalization pathway in the porphyrin ring can serve to explain the upfield bias of the pyrrole proton signal in that positive π-spin density at the β-pyrrole carbon position results in an upfield contribution for the attached proton. Presence of an anionic axial ligand is not necessarily associated with this upfield bias of the pyrrole proton signal (compare the value of 61.0 ppm for the mercaptide complex), but a small basic axial ligand may be responsible for the effect.

Acknowledgment. Support from National Science Foundation Grant CHE 83-17451 is gratefully acknowledged.

Contribution from the Department of Chemistry and Centre for Chemical Physics, The University of Western Ontario, London, Ontario N6A 5B7, Canada, Canadian Synchrotron Radiation Facility, Synchrotron Radiation Center, University of Wisconsin, Stoughton, Wisconsin 53589, and Division of Chemistry, National Research Council of Canada, Ottawa, Ontario K1A 0R9, Canada

Variable-Energy Photoelectron Study of the Valence Levels of $Si(CH_3)_4$ and $Sn(CH_3)_4$ and the Sn 4d Levels of $Sn(CH_3)_4$

J. E. Bice, K. H. Tan, G. M. Bancroft,* and J. S. Tse†

Received April 8, 1987

By the use of monochromatized synchrotron radiation, the gas-phase photoelectron spectra of the valence levels of $Si(CH_3)_4$ and the valence and Sn 4d levels of $Sn(CH_3)_4$ have been obtained and compared between 21- and 70-eV photon energies. For both molecules, experimental valence-band branching ratios have been obtained and compared with theoretical branching ratios from MS-Xα calculations. The generally good agreement obtained between experiment and theory confirms the orbital assignment: $3t_2 < 1t_1 \simeq 1e \simeq 2t_2 < 2a_1$, in order of increasing binding energy. The theoretical and experimental results for both molecules are remarkably similar. For both $Si(CH_3)_4$ and $Sn(CH_3)_4$, resonances were predicted at ~4-, ~10-, and ~20-eV kinetic energies. The predicted resonance positions are in good agreement with experimental results for the high-energy resonance. In conjunction with other recent results on shape resonances in analogous large molecules (e.g. CF_4, SiF_4, SF_6, and SeF_6), these results indicate that shape resonance behavior for other than first-row central atoms (e.g. C) is determined mainly by the nature and symmetry of the ligands and that the resonances are not very sensitive to the detailed molecular potential. Interchannel coupling with Sn 4d photoemission is important for the outermost $3t_2$ orbital of $Sn(CH_3)_4$. The Sn $4d_{5/2}$:$4d_{3/2}$ ratio of $Sn(CH_3)_4$ deviates significantly from the statistical value of 1.5 in the low photon energy region.

Introduction

The tetramethyl compounds of group IV (14) (C, Si, Ge, Sn, Pb) elements have been the subject of a number of ultraviolet photoelectron studies.[1-6] These studies have primarily involved the assignment of the outer valence levels and, in particular, the location of the $2a_1$ and $3t_2$ metal-carbon bonding orbitals. The question of d-level participation in bonding has been widely debated in discussing the electronic structure of these compounds.[5,7-11]

In this study, we have obtained gas-phase photoelectron spectra of the valence levels of $Si(CH_3)_4$ and $Sn(CH_3)_4$ as a function of photon energy from 21 to 70 eV. We were able to include in our study the $1a_1$ and $1t_2$ molecular orbitals of primarily C 2s character that were inaccessible in previous He I photoelectron studies. We had four objectives: First, we expected that our study would confirm the valence-band assignment through a comparison of experimental branching ratios (BR's) with theoretical BR's obtained from MS-Xα calculations. Second, we wanted to examine the valence-band branching ratios for evidence of molecular shape resonances and to compare the shape resonance behaviors for the two analogous molecules. In a previous study, large differences in resonance behavior were observed between CF_4 and SiF_4.[12] The study of $Si(CH_3)_4$ was of particular interest since it is isoelectronic with SiF_4 and the valence band cross sections of SiF_4 exhibit a number of shape resonances.[12] Such resonances have been observed above the Si 2p threshold in absorption spectra of both SiF_4[13-17] and $Si(CH_3)_4$.[18] Third, we wanted to investigate further the role of core-level intershell coupling on valence-level cross

* To whom correspondence should be addressed at The University of Western Ontario.
† NRCC No. 28029.

(1) Bock, H.; Ensslin, W. *Angew. Chem., Int. Ed. Engl.* **1971**, *10*, 404.
(2) Green, M. C.; Lappert, M. F.; Pedley, J. B.; Schmidt, W.; Wilkins, B. T. *J. Organomet. Chem.* **1971**, *31*, C55.
(3) Evans, S.; Green, J. C.; Joachim, P. J.; Orchard, A. F.; Turner, D. W.; Maier, J. P. *J. Chem. Soc., Faraday Trans. 2* **1972**, *68*, 905.
(4) Jonas, A. E.; Schweitzer, G. K.; Grimm, F. A.; Carlson, T. A. *J. Electron Spectrosc. Relat. Phenom.* **1972/1973**, *1*, 29.
(5) Boschi, R.; Lappert, M. F.; Pedley, J. B.; Schmidt, W.; Wilkins, B. T. *J. Organomet. Chem.* **1973**, *50*, 69.
(6) Bancroft, G. M.; Pellach, E.; Tse, J. S. *Inorg. Chem.* **1982**, *21*, 2950.
(7) Perry, W. B.; Jolly, W. L. *J. Electron Spectrosc. Relat. Phenom.* **1974**, *4*, 219.
(8) Perry, W. B.; Jolly, W. L. *Chem. Phys. Lett.* **1972**, *17*, 611.
(9) Toman, J. J.; Frost, A. A.; Topiol, S.; Jacobson, S.; Ratner, M. A. *Theor. Chim. Acta* **1981**, *58*, 285.
(10) Berkovitch-Yellin, Z.; Ellis, D. E.; Ratner, M. A. *Chem. Phys.* **1981**, *62*, 21.
(11) Bertoncello, R.; Daudey, J. P.; Granozzi, G.; Russo, U. *Organometallics* **1986**, *5*, 1866.
(12) Yates, B. W.; Tan, K. H.; Bancroft, G. M.; Coatsworth, L. L. *J. Chem. Phys.* **1985**, *83*, 4906.
(13) Zimkina, T. M.; Vinogradov, A. S. *J. Phys. (Les Ulis, Fr.)* **1971**, *32*, C43.
(14) Vinogradov, A. S.; Zimkina, T. M. *Opt. Spectrosc. (Engl. Transl.)* **1971**, *31*, 288.
(15) Hayes, W.; Brown, F. C. *Phys. Rev. A* **1971**, *6*, 21.
(16) Friedrich, H.; Pittel, B.; Kabe, P.; Schwartz, W. H. E.; Sonntag, B. *J. Phys. B* **1980**, *13*, 25.
(17) Pavlychev, A. A.; Vinogradov, A. S.; Zimkina, T. M. *Opt. Spectrosc. (Engl. Transl.)* **1982**, *52*, 139.
(18) Sodhi, R. N. S.; Daviel, S.; Brion, C. E.; de Souza, G. G. B. *J. Electron Spectrosc. Relat. Phenom.* **1985**, *35*, 45.

0020-1669/87/1326-4106$01.50/0

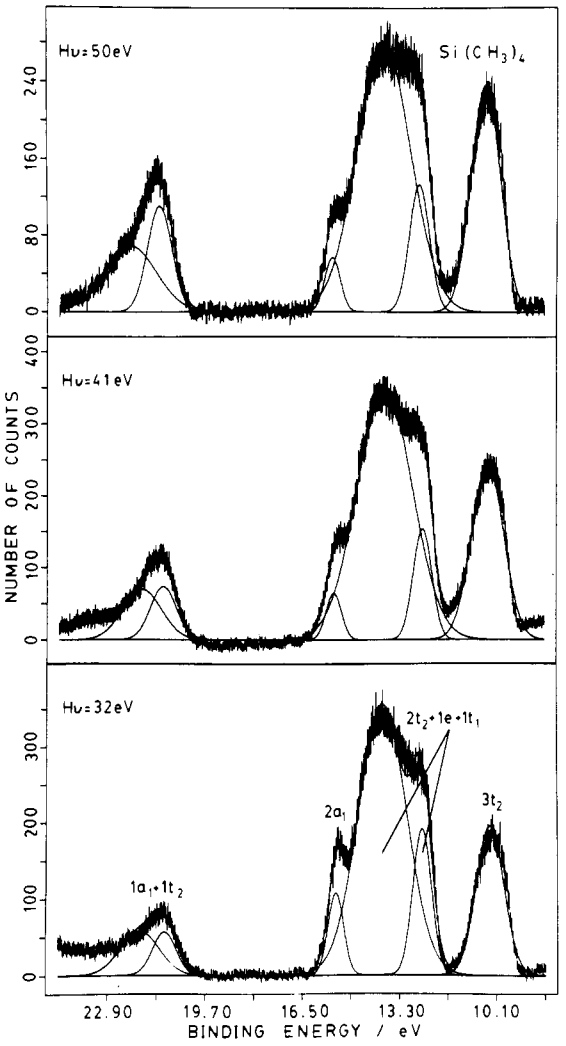

Figure 1. Photoelectron spectra of $Si(CH_3)_4$ at 32-, 41-, and 50-eV photon energy. The molecular orbital assignment is given in the bottom plot.

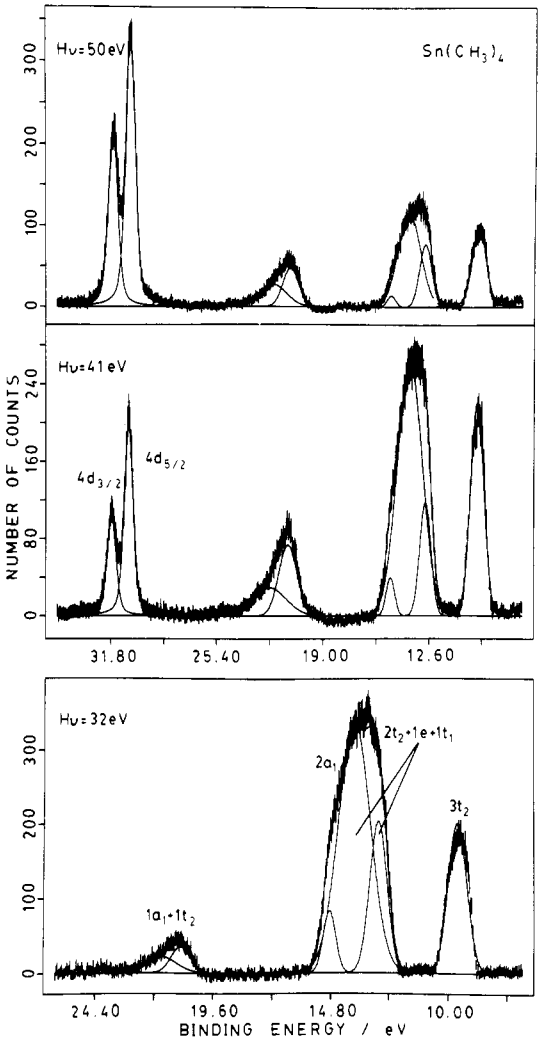

Figure 2. Photoelectron spectra of $Sn(CH_3)_4$ at 32-, 41-, and 50-eV photon energy. The molecular orbital assignment is given in the lower plots.

sections[19-21] by examining the valence-level branching ratios of $Sn(CH_3)_4$ on scanning across the Sn 4d threshold. Finally, we also wanted to report the Sn 4d branching ratio from 36- to 100-eV photon energy and discuss the results in terms of the influence of the chemical environment. After this paper was submitted, an experimental synchrotron radiation study of $Sn(CH_3)_4$ appeared,[22] and we compare our results with Novak et al.[22]

Experimental Section

The gas-phase photoelectron spectra of $Si(CH_3)_4$ and $Sn(CH_3)_4$ were obtained by using photons from the Canadian Synchrotron Radiation Facility (CSRF)[23,24] at Tantalus I, an electron storage ring operated by the University of Wisconsin at Stoughton, WI. All photoelectron spectra were recorded at the "magic angle" by using the spectrometer and gas-inlet system described in detail in previous papers.[12,19,25] The tetramethylsilane (NMR grade, 99.97% purity) and tetramethyltin (99.5% purity) were obtained commercially from the Alfa Division, Ventron Corp. Each sample was degassed through several cycles of freezing and pumping and used without further purification. The tetramethyltin sample required gentle heating in order to maintain a stable backing pressure. A 600 line mm^{-1} holographic grating was used, which limited our minimum photon energy to 21 eV. The valence-band spectra were recorded at a 50-eV electron analyzer pass energy (0.4-eV electron resolution) from 21- to 70-eV photon energy. The Sn 4d levels of $Sn(CH_3)_4$ were recorded out to 100 eV. The monochromator resolution ranged from 300-μm slits (2.4-Å photon resolution) below 50-eV photon energy to 80-μm slits (0.6-Å photon resolution) at 100-eV photon energy. Spectra were taken at intervals of 1–2 eV from 21 to 50 eV and every 3–5 eV above 50 eV. The transmission function of the electron spectrometer has been found to be constant to within 20% for kinetic energies between 2 and 60 eV,[26] enabling the determination of branching ratios without intensity corrections.

All spectra were fitted to combination Lorentzian–Gaussian peak shapes by using an iterative procedure described previously.[27] Branching ratios [(area/sum of areas) × 100] can then be obtained. However, many of the peaks strongly overlap (Figures 1 and 2), and accurate branching ratios can only be strictly obtained for well-resolved peaks or bands because photoelectron peaks are often quite asymmetric due to vibrational effects (see for example, ref 28). We have obtained semiquantitative branching ratios for the $2a_1$ orbital in both compounds by constraining the widths to be 0.60 eV in both cases and constraining the positions at the same value for all spectra (vide infra). This branching

(19) Yates, B. W.; Tan, K. H.; Bancroft, G. M.; Tse, J. S. *J. Chem. Phys.* **1986**, *85*, 3840.
(20) Lefebvre-Brion, H.; Raseev, G.; Le Rouzo, H. *Chem. Phys. Lett.* **1986**, *123*, 341.
(21) Bice, J. E.; Tan, K. H.; Bancroft, G. M.; Yates, B. W.; Tse, J. S. *J. Chem. Phys.* **1987**, *87*, 821.
(22) Novak, I.; Benson, J. M.; Svensson, A.; Potts, A. W. *Chem. Phys. Lett.* **1987**, *135*, 471.
(23) Tan, K. H.; Bancroft, G. M.; Coatsworth, L. L.; Yates, B. W. *Can. J. Phys.* **1982**, *60*, 131.
(24) Tan, K. H.; Cheng, P. C.; Bancroft, G. M.; McGowan, J. W. *Can. J. Spectrosc.* **1984**, *29*, 134.
(25) Yates, B. W.; Tan, K. H.; Coatsworth, L. L.; Bancroft, G. M. *Phys. Rev. A* **1985**, *31*, 1529.
(26) Aksela, S.; Tan, K. H.; Bancroft, G. M.; Aksela, H.; Yates, B. W.; Coatsworth, L. L. *Phys. Rev. A* **1985**, *32*, 1219.
(27) Bancroft, G. M.; Adams, I.; Coatsworth, L. L.; Bennewitz, C. O.; Brown, J. D.; Westwood, W. D. *Anal. Chem.* **1975**, *47*, 586.
(28) Mehaffy, D.; Keller, P. R.; Taylor, J. W.; Carlson, T. A.; Grimm, F. A. *J. Electron. Spectrosc. Relat. Phenom.* **1983**, *28*, 239.

Table I. Parameters Used in the MS-Xα Calculation of $Si(CH_3)_4$ and $Sn(CH_3)_4$

region	x	y	z^a	R^a	α	l_{max} initial state	l_{max} final state
outer sphere	0.0	0.0	0.0	5.730	0.7620	3	6
Si	0.0	0.0	0.0	2.360	0.7275	2	3
C_1	0.0	2.9007	2.0511	1.900	0.7593	1	2
C_2	2.9007	0.0	−2.0511	1.900	0.7593	1	2
C_3	0.0	−2.9007	2.0511	1.900	0.7593	1	2
C_4	−2.9007	0.0	−2.0511	1.900	0.7593	1	2
H_{11}	0.0	2.3401	4.0332	1.068	0.7772	0	1
H_{12}	1.6818	4.0220	1.6547	1.068	0.7772	0	1
H_{13}	−1.6818	4.0220	1.6547	1.068	0.7772	0	1
H_{21}	2.3401	0.0	−4.0332	1.068	0.7772	0	1
H_{22}	4.0220	1.6818	−1.6547	1.068	0.7772	0	1
H_{23}	4.0220	−1.6818	−1.6547	1.068	0.7772	0	1
H_{31}	0.0	−2.3401	4.0332	1.068	0.7772	0	1
H_{32}	1.6818	−4.0220	1.6547	1.068	0.7772	0	1
H_{33}	−1.6818	−4.0220	1.6547	1.068	0.7772	0	1
H_{41}	−2.3401	0.0	−4.0332	1.068	0.7772	0	1
H_{42}	−4.0220	−1.6818	1.6547	1.068	0.7772	0	1
H_{43}	−4.0220	1.6818	−1.6547	1.068	0.7772	0	1
outer sphere	0.0	0.0	0.0	6.260	0.7587	3	6
Sn	0.0	0.0	0.0	3.000	0.7007	2	3
C_1	0.0	3.3636	2.3784	1.944	0.7592	1	2
C_2	3.3636	0.0	−2.3784	1.944	0.7592	1	2
C_3	0.0	−3.3636	2.3784	1.944	0.7592	1	2
C_4	−3.3636	0.0	−2.3784	1.944	0.7592	1	2
H_{11}	0.0	2.8030	4.3605	1.068	0.7772	0	1
H_{12}	1.6818	4.4849	1.9820	1.068	0.7772	0	1
H_{13}	−1.6818	4.4849	1.9820	1.068	0.7772	0	1
H_{21}	2.8030	0.0	−4.3605	1.068	0.7772	0	1
H_{22}	4.4849	1.6818	−1.9820	1.068	0.7772	0	1
H_{23}	4.4849	−1.6818	−1.9820	1.068	0.7772	0	1
H_{31}	0.0	−2.8030	4.3605	1.068	0.7772	0	1
H_{32}	1.6818	−4.4849	1.9820	1.068	0.7772	0	1
H_{33}	−1.6818	−4.4849	1.9820	1.068	0.7772	0	1
H_{41}	−2.8030	0.0	−4.3605	1.068	0.7772	0	1
H_{42}	−4.4849	1.6818	−1.9820	1.068	0.7772	0	1
H_{43}	−4.4849	−1.6818	−1.9820	1.068	0.7772	0	1

[a] Coordinates and sphere radii in au.

ratio was not determined in the previous study,[22] and it is important for our discussion of resonances on these compounds.

Theory

Theoretical partial cross sections were obtained for the valence levels of $Si(CH_3)_4$ and the valence and Sn 4d levels of $Sn(CH_3)_4$ as a function of photon energy, by using the MS-Xα cross section program of Davenport.[29,30] These calculations were performed on an IBM 3081 computer located at the National Research Council of Canada Computing Centre in Ottawa. The parameters employed in the calculations are given in Table I. The atomic exchange parameters, α_{HF}, are those of Schwarz.[31,32] A weighted average of the atomic exchange parameters based on the number of valence electrons was used for the outer-sphere and intersphere regions. Atomic spheres were allowed to overlap by 10% in the $Si(CH_3)_4$ calculation and by 20% in the $Sn(CH_3)_4$ calculation. Bond lengths of 1.88, 2.18, and 1.09 Å were used for the Si–C, Sn–C, and C–H bonds, respectively.[33,34] The four methyl groups were assumed to have idealized tetrahedral geometry in each molecule. Although the coordinates shown in Table I reflect the T_d symmetry about the central atom, the calculation was performed by assuming C_{2v} symmetry for simplicity. A kinetic energy mesh size of 1.36 eV was used in the calculation of photoionization cross sections.

The photoionization cross sections were calculated with the converged ground-state SCF potential modified with a Latter tail[35] to correct for large-r behavior. In order to define the final state properly, the spherical harmonics were extended to higher azimuthal l quantum numbers as indicated in Table I. Previous studies have shown that the numerical results are sensitive to the completeness of the partial wave expansion of the continuum state.[36,37] All symmetry-allowed processes based on the dipolar selection rule were included in the calculation.

Results and Discussion

Representative spectra for $Si(CH_3)_4$ and $Sn(CH_3)_4$ at 32-, 41-, and 50-eV photon energies are shown in Figures 1 and 2, respectively. The outer two bands in the photoelectron spectra of each compound show resolution similar to that observed in previous He I photoelectron studies.[2-4] The molecular orbital assignment given in Figures 1 and 2 is in agreement with the results of previous extended Hückel[7] and ab initio calculations.[9-11]

The well-separated photoelectron band at lowest binding energy in the spectra of both $Si(CH_3)_4$ and $Sn(CH_3)_4$ is readily assigned to the $3t_2$ molecular orbital. This is a metal–carbon bonding orbital. The broad photoelectron band centered at ~13.3 eV contains ionizations from the methyl carbon–hydrogen bonding orbitals ($2t_2 + 1e + 1t_1$) that are not resolved. The $2a_1$ molecular orbital, which is well-resolved at 15.5 eV in $Si(CH_3)_4$ spectra, only appears as a shoulder on the high binding energy side of the second band in $Sn(CH_3)_4$ spectra. This is also a metal–carbon bonding orbital. The photoelectron band at ~21.7 eV, which had previously been observed in an X-ray photoelectron study[7] of gaseous

(29) Davenport, J. W. Ph.D. Thesis, University of Pennsylvania, 1976.
(30) Davenport, J. W. *Phys. Rev. Lett.* **1976**, *36*, 945.
(31) Schwarz, K. *Phys. Rev. B: Solid State* **1972**, *5*, 2466.
(32) Schwarz, K. *Theor. Chim. Acta* **1974**, *34*, 225.
(33) Beagley, B.; Monaghan, J. J.; Hewitt, T. G. *J. Mol. Struct.* **1971**, *8*, 401.
(34) Nagashima, M.; Fujii, H.; Kimura, M. *Bull. Chem. Soc. Jpn.* **1973**, *46*, 3708.
(35) Latter, R. *Phys. Rev.* **1955**, *99*, 510.
(36) Roche, M.; Salahub, D. R.; Messmer, R. P. *J. Electron Spectrosc. Relat. Phenom.* **1980**, *19*, 273.
(37) Grimm, F. A.; Carlson, T. A.; Dress, W. B.; Agron, P.; Thomson, J. O.; Davenport, J. W. *J. Chem. Phys.* **1978**, *72*, 3041.

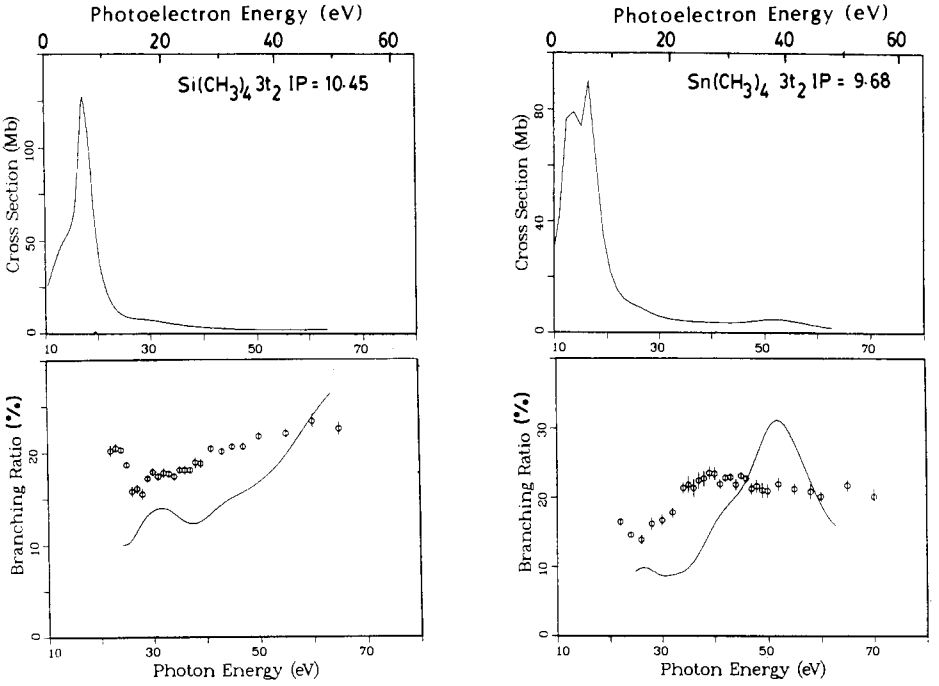

Figure 3. Experimental branching ratios and theoretical MS-Xα cross sections (σ) and branching ratios (solid lines) for the photoionization of the $3t_2$ orbital of $Si(CH_3)_4$ and $Sn(CH_3)_4$.

$Si(CH_3)_4$, is assigned to ionizations from the $1a_1$ and $1t_2$ molecular orbitals. These orbitals consist primarily of C 2s character. The $4d_{5/2}$ and $4d_{3/2}$ spin–orbit components of the Sn 4d levles were observed at 30.7 and 31.8 eV, respectively, in the spectra of $Sn(CH_3)_4$.

Branching ratios were determined from the fitted peak areas. A two-peak fit of the broad, asymmetric band at ~13.3 eV was required in order to accurately determine its area. The width of the photoelectron peak corresponding to ionization from the $2a_1$ orbital in $Sn(CH_3)_4$ was approximated by that found for the reasonably well-resolved $2a_1$ peak in $Si(CH_3)_4$ (0.60 eV). From the fitted spectra of $Sn(CH_3)_4$, the position of the $2a_1$ level was found to be 14.9 eV. This is in good agreement with the results of a recent pseudopotential ab initio calculation placing this orbital at 14.48 eV.[9] The area of the $1a_1 + 1t_2$ band in the photoelectron spectra of $Si(CH_3)_4$ was accurately determined from separate fits of this band in which the sloping base line at lower photon energies (due to the scattering of secondary electrons of low kinetic energies) was taken into account.

Since the total absorption cross sections for $Si(CH_3)_4$ and $Sn(CH_3)_4$ are not known in the 21–70-eV range, the experimental branching ratios were not converted to partial cross sections. Therefore, experimental branching ratios were compared wtih theoretical branching ratios obtained from cross sections calculated for $Si(CH_3)_4$ and $Sn(CH_3)_4$ by the MS-Xα method. In the previous study on $Sn(CH_3)_4$,[22] the branching ratios were converted to cross sections by using the atomic Sn 4d cross sections.[38] We prefer not to use this procedure for two reasons. First, it can only be used accurately above about 40 eV.[22,38] Second, recent theoretical[39] and experimental[21,40] results indicate that molecular d cross sections can be quite different from atomic values.

The theoretical partial cross sections (σ) and the theoretical and experimental branching ratios for the valence molecular orbitals of $Si(CH_3)_4$ and $Sn(CH_3)_4$ are illustrated in Figures 3–6. The theoretical and experimental branching ratios for the valence orbitals of $Sn(CH_3)_4$ have been calculated with the exclusion of the Sn 4d levels to allow a direct comparison of the results between $Si(CH_3)_4$ and $Sn(CH_3)_4$. In order to facilitate future conversion of the branching ratios to partial cross sections, the experimental branching ratios, including the Sn 4d levels in the $Sn(CH_3)_4$ data, are presented in Tables II and III. The errors obtained are derived from the fitted peak areas. Both the theoretical and experimental valence-band cross sections and branching ratios are remarkably similar for the two compounds, and the experimental and theoretical branching ratios are in qualitative agreement for all orbitals for both compounds. Our $Sn(CH_3)_4$ branching ratios are in good agreement with previous results[22] although the previous study did not resolve the $2a_1$ orbital.[22]

In photoelectron[41] and electron-impact[18] studies of $Si(CH_3)_4$ above the Si 2p threshold, two resonances have been observed. These resonances were considered to be due to resonant trapping

Table II. Experimental Branching Ratios for the Outer Orbitals of $Si(CH_3)_4$ as a Function of Photon Energy

	branching ratio			
$h\nu$, eV	$1a_1 + 1t_2$	$2a_1$	$2t_2 + 1e + 1t_1$	$3t_2$
22.0		2.0 ± 0.3	77.7 ± 2.8	20.2 ± 0.6
23.0		1.9 ± 0.2	77.6 ± 2.0	20.5 ± 0.5
24.0		1.8 ± 0.2	77.8 ± 1.4	20.3 ± 0.3
25.0		3.2 ± 0.2	78.1 ± 1.9	18.7 ± 0.4
26.0	2.2 ± 0.2	4.1 ± 0.4	77.8 ± 3.3	15.8 ± 0.6
27.0	3.8 ± 0.1	4.0 ± 0.4	76.1 ± 2.3	16.1 ± 0.5
28.0	3.5 ± 0.2	4.8 ± 0.4	76.1 ± 3.0	15.5 ± 0.6
29.0	5.4 ± 0.2	5.6 ± 0.3	71.8 ± 1.4	17.2 ± 0.4
30.0	4.3 ± 0.2	4.1 ± 0.3	73.8 ± 1.8	17.9 ± 0.4
31.0	7.9 ± 0.2	4.9 ± 0.3	69.8 ± 1.8	17.4 ± 0.4
32.0	8.1 ± 0.3	5.5 ± 0.4	68.6 ± 2.1	17.8 ± 0.5
33.0	8.9 ± 0.2	4.9 ± 0.3	68.5 ± 2.0	17.7 ± 0.4
34.0	9.5 ± 0.3	4.6 ± 0.3	67.5 ± 1.6	18.4 ± 0.4
35.0	10.3 ± 0.3	4.6 ± 0.3	67.0 ± 1.9	18.1 ± 0.4
36.0	10.7 ± 0.4	5.0 ± 0.4	66.2 ± 2.3	18.1 ± 0.5
37.0	12.6 ± 0.3	3.9 ± 0.3	65.4 ± 1.8	18.1 ± 0.4
38.0	10.8 ± 0.4	4.2 ± 0.4	66.2 ± 2.5	18.9 ± 0.6
39.0	14.3 ± 0.4	3.4 ± 0.3	63.5 ± 2.2	18.8 ± 0.5
41.0	11.6 ± 0.3	2.8 ± 0.4	65.1 ± 1.6	20.4 ± 0.4
43.0	18.0 ± 0.4	2.6 ± 0.2	59.3 ± 1.7	20.1 ± 0.4
45.0	16.6 ± 0.5	2.6 ± 0.2	60.2 ± 1.3	20.6 ± 0.4
47.0	18.4 ± 0.5	2.3 ± 0.2	58.7 ± 1.6	20.6 ± 0.4
50.0	18.5 ± 0.6	2.7 ± 0.2	57.0 ± 1.8	21.7 ± 0.5
55.0	22.3 ± 0.7	2.9 ± 0.2	52.8 ± 2.2	22.0 ± 0.5
60.0	24.2 ± 1.0	2.4 ± 0.4	50.1 ± 3.3	23.3 ± 0.8
65.0	24.8 ± 0.9	2.4 ± 0.3	50.4 ± 1.6	22.5 ± 0.7

(38) Gerard, P.; Krause, M. O.; Carlson, T. A. Z. Physik D2 **1986**, 123.
(39) Tambe, B. R.; Manson, G. T. *Phys. Rev. A* **1984**, *30*, 256.
(40) Gurtler, K.; Tan, K. H.; Bancroft, G. M.; Norton, P. R. *Phys. Rev. B: Condens. Matter* **1987**, *35*, 6024.
(41) de Souza, G. G. B.; Morin, P.; Nenner, I. J. *Chem. Phys.* **1985**, *83*, 492.

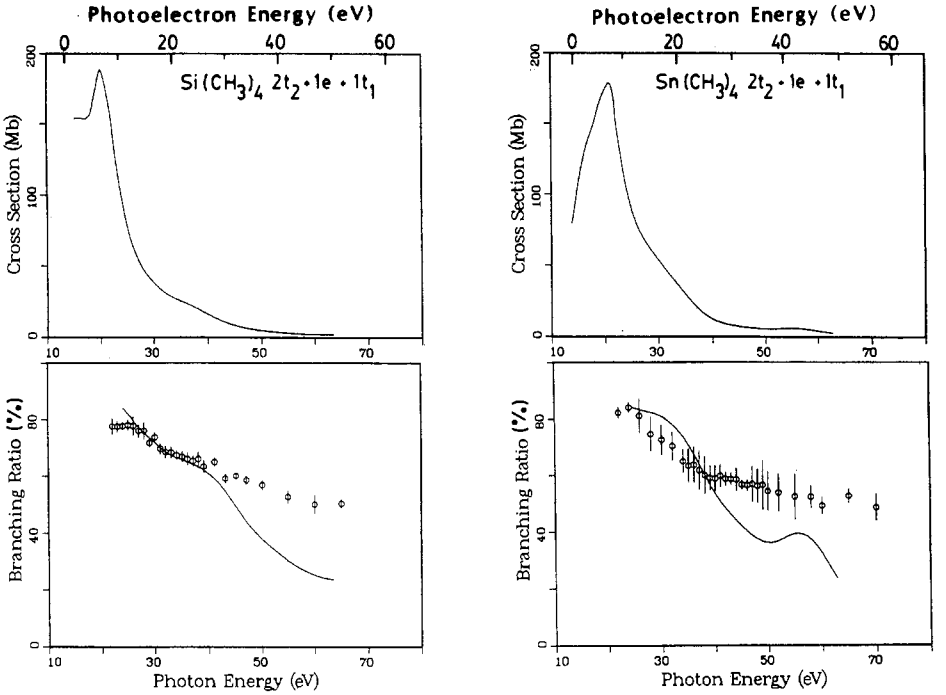

Figure 4. Experimental branching ratios and theoretical MS-Xα cross sections (σ) and branching ratios (solid lines) for the photoionization of the $1t_1$, 1e, and $2t_2$ orbitals of $Si(CH_3)_4$ and $Sn(CH_3)_4$.

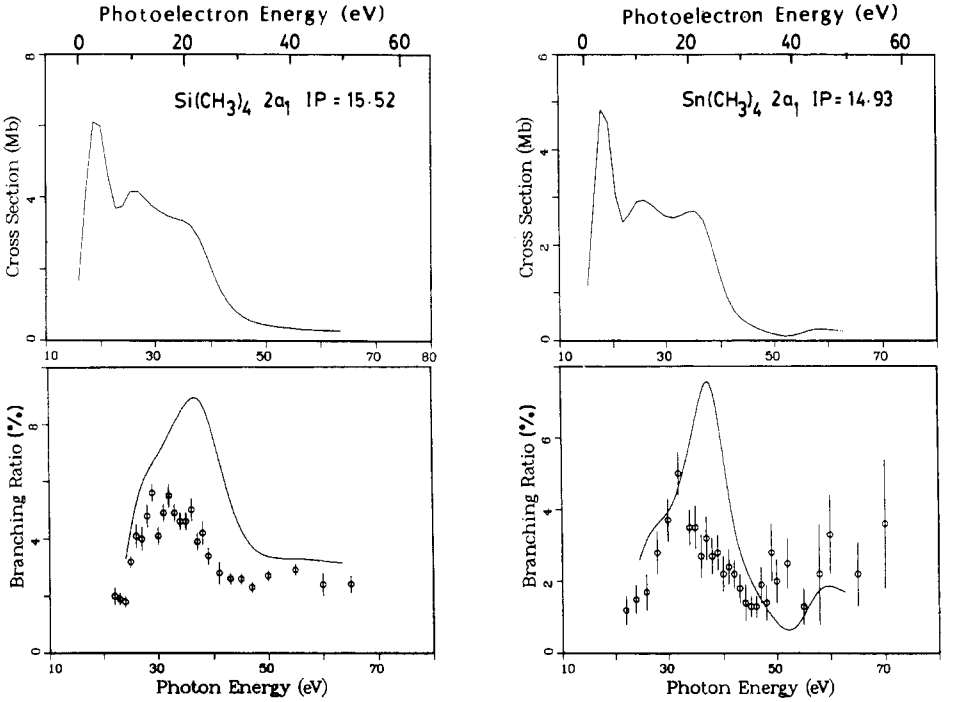

Figure 5. Experimental branching ratios and theoretical MS-Xα cross sections (σ) and branching ratios (solid lines) for the photoionization of the $2a_1$ orbital of $Si(CH_3)_4$ and $Sn(CH_3)_4$.

by a potential barrier of primarily d character. The intense resonance near threshold was assigned to an e exit channel, while a much weaker resonance located at ~18 eV above threshold was assigned to a t_2 exit channel. In addition, a recent photoabsorption study[42] of $Si(CH_3)_4$ near the Si 1s edge indicated the presence of a t_2 shape resonance 6.0 eV above this edge. Evidence of this resonance has also been found in a recent high-resolution photoabsorption study of $Si(CH_3)_4$ above the Si 2p threshold.[43]

The results for the highest occupied molecular orbital, $3t_2$, of $Si(CH_3)_4$ and $Sn(CH_3)_4$ are presented in Figure 3. From the MS-Xα calculations, this metal–carbon bonding orbital is composed of mainly C 2p (57%) and either Si 3p (25%) or Sn 5p (29%) character. For both molecules, the calculations indicated the presence of ~6% d character in this orbital. After low energy shape resonances, the rapid decline in partial cross section toward higher photon energies is characteristic of the high percentage of p character in this orbital.[44]

Since both e and t_2 exit channels are dipole-allowed for a molecular orbital of t_2 symmetry and since the $3t_2$ molecular orbital of Me_4M compounds contains appreciable central atom p char-

(42) Bodeur, S.; Nenner, J.; Millie, P. *Phys. Rev. A* **1986**, *34*, 2986.
(43) Bozek, J.; Tan, K. H.; Bancroft, G. M., to be submitted for publication.
(44) Price, W. C.; Potts, A. W.; Streets, D. G. In *Electron Spectroscopy*; Shirley, D. A., Ed.; North-Holland: Amsterdam, 1972.

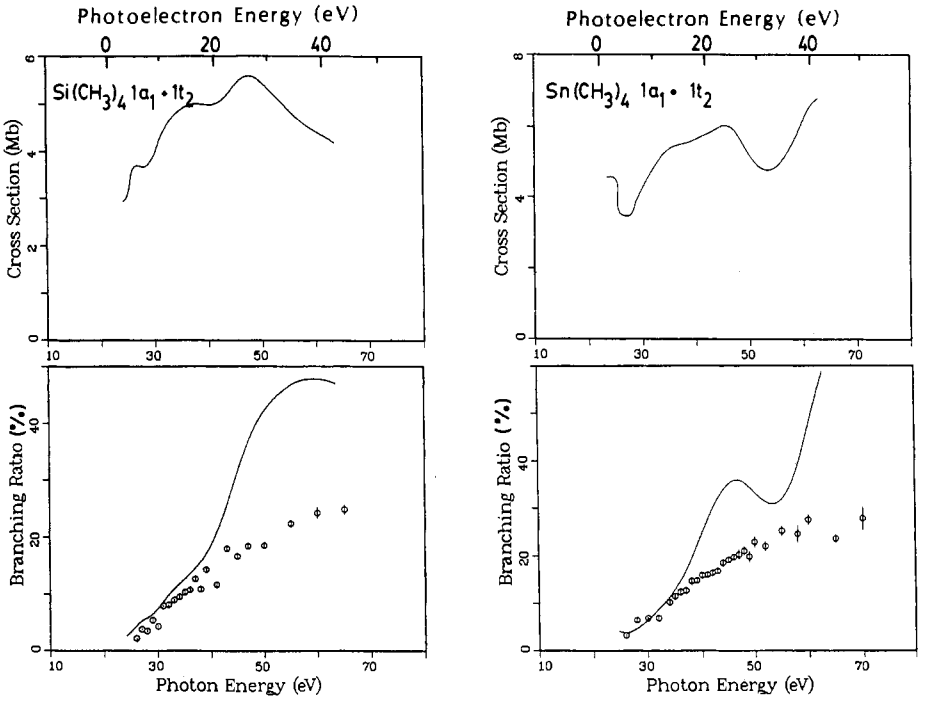

Figure 6. Experimental branching ratios and theoretical MS-Xα cross sections (σ) and branching ratios (solid lines) for the photoionization of the $1t_2$ and $1a_1$ orbitals of $Si(CH_3)_4$ and $Sn(CH_3)_4$.

Table III. Experimental Branching Ratios for the Outer Orbitals of $Sn(CH_3)_4$ as a Function of Photon Energy

	branching ratio					
$h\nu$, eV	$4d_{3/2}$	$4d_{5/2}$	$1a_1 + 1t_2$	$2a_1$	$2t_2 + 1e + 1t_1$	$3t_2$
22.0				1.2 ± 0.4	82.2 ± 1.9	16.5 ± 0.4
24.0				1.5 ± 0.4	84.0 ± 1.8	14.6 ± 0.3
26.0			3.2 ± 0.3	1.7 ± 0.5	81.1 ± 5.9	13.9 ± 0.7
28.0			6.4 ± 0.4	2.8 ± 0.6	74.6 ± 6.1	16.2 ± 0.9
30.0			6.8 ± 0.4	3.7 ± 0.6	72.8 ± 5.3	16.7 ± 0.8
32.0			6.8 ± 0.4	5.0 ± 0.6	70.4 ± 5.0	17.8 ± 0.8
34.0			10.1 ± 0.5	3.5 ± 0.5	65.0 ± 4.1	21.3 ± 0.8
35.0			11.4 ± 0.7	3.5 ± 0.6	63.4 ± 6.0	21.8 ± 1.2
36.0	3.9 ± 0.4	8.4 ± 0.5	10.8 ± 0.7	2.4 ± 0.5	55.9 ± 5.8	18.7 ± 1.1
37.0	5.9 ± 0.4	12.8 ± 0.7	10.2 ± 0.6	2.6 ± 0.5	50.2 ± 5.5	18.2 ± 1.0
38.0	7.1 ± 0.5	14.3 ± 0.8	11.5 ± 0.6	2.1 ± 0.4	47.2 ± 5.2	17.9 ± 0.9
39.0	7.8 ± 0.4	14.6 ± 0.6	11.4 ± 0.5	2.2 ± 0.4	45.8 ± 3.4	18.2 ± 0.7
40.0	8.6 ± 0.3	15.0 ± 0.5	11.9 ± 0.5	1.7 ± 0.4	44.9 ± 3.4	17.9 ± 0.7
41.0	6.7 ± 0.3	12.9 ± 0.4	12.8 ± 0.5	1.9 ± 0.4	48.1 ± 3.3	17.6 ± 0.6
42.0	9.8 ± 0.2	16.6 ± 0.4	12.0 ± 0.4	1.6 ± 0.3	43.2 ± 1.8	16.8 ± 0.4
43.0	10.7 ± 0.2	17.4 ± 0.3	12.0 ± 0.4	1.3 ± 0.3	42.2 ± 1.5	16.5 ± 0.4
44.0	13.6 ± 0.4	21.7 ± 0.6	11.9 ± 0.5	0.9 ± 0.3	37.8 ± 2.6	14.1 ± 0.5
45.0	13.5 ± 0.2	22.4 ± 0.3	12.2 ± 0.3	0.8 ± 0.2	36.3 ± 1.0	14.8 ± 0.3
46.0	14.6 ± 0.2	23.2 ± 0.4	12.2 ± 0.3	0.8 ± 0.2	35.0 ± 1.2	14.1 ± 0.3
47.0	16.2 ± 0.6	26.2 ± 0.9	11.6 ± 0.6	1.1 ± 0.3	32.7 ± 3.6	12.2 ± 0.5
48.0	16.0 ± 0.6	26.6 ± 0.9	12.0 ± 0.5	0.8 ± 0.3	32.3 ± 3.4	12.4 ± 0.5
49.0	17.7 ± 0.8	29.4 ± 1.3	10.4 ± 0.6	1.5 ± 0.4	29.9 ± 4.6	11.1 ± 0.6
50.0	19.2 ± 0.7	29.9 ± 1.1	11.6 ± 0.6	1.0 ± 0.3	27.6 ± 3.5	10.6 ± 0.5
52.0	21.0 ± 0.7	34.0 ± 1.1	9.8 ± 0.5	1.1 ± 0.3	24.1 ± 3.0	9.8 ± 0.4
55.0	23.8 ± 0.8	36.5 ± 1.2	10.0 ± 0.4	0.5 ± 0.2	20.8 ± 3.2	8.4 ± 0.3
58.0	29.9 ± 0.6	42.4 ± 0.8	6.8 ± 0.5	0.6 ± 0.4	14.5 ± 1.1	5.8 ± 0.3
60.0	30.5 ± 0.4	42.6 ± 0.6	7.4 ± 0.3	0.9 ± 0.3	13.2 ± 0.8	5.4 ± 0.2
65.0	31.4 ± 0.4	45.6 ± 0.6	5.4 ± 0.2	0.5 ± 0.2	12.1 ± 0.6	5.0 ± 0.2
70.0	34.4 ± 0.6	48.7 ± 0.8	4.7 ± 0.4	0.6 ± 0.3	8.2 ± 0.8	3.4 ± 0.2

acter, the partial cross sections and branching ratios of this orbital of $Si(CH_3)_4$ and $Sn(CH_3)_4$ were examined for evidence of these resonances. The presence of resonances at kinetic energies between 4 and 7 eV for both $Si(CH_3)_4$ and $Sn(CH_3)_4$ was indicated by the MS-Xα results (Figure 3), since the resonance criteria of Kreile et al.[45] were met (see Table IV). The MS-Xα results indicated that these resonances were consistent with t_2 and e exit channels. The position of the t_2 resonance (6.0 eV) found in recent photoabsorption studies near the Si 1s and 2p edges of $Si(CH_3)_4$ is in reasonable agreement with the valence results. Unfortunately, the monochromator limited our minimum photon energy to 21 eV and we were not able to examine the $3t_2$ branching ratios close to threshold. However, the decline in $3t_2$ experimental branching ratio for both $Si(CH_3)_4$ and $Sn(CH_3)_4$ to a minimum at ~26-eV photon energy and an increase below this suggest the presence of a resonance. These spectra now need to be recorded between 10- and 20-eV photon energy to confirm the low energy resonances.

For the $3t_2$ orbital of $Si(CH_3)_4$, the theoretical branching ratios are in reasonable agreement with experiment. Somewhat poorer agreement is obtained between the corresponding results for the $3t_2$ orbital of $Sn(CH_3)_4$. However, for both $Si(CH_3)_4$ and Sn-

(45) Kreile, J.; Schweig, A.; Thiel, W. *Chem. Phys. Lett.* **1984**, *108*, 259.

Table IV. Theoretical MS–Xα Eigenphase Sum Features

molecule	MO	channel symm	MS–Xα results: E_{phase},[a] eV	Δ(eigenphase sum)[b]	E_{cross}, eV
$Si(CH_3)_4$	$3t_2$	e, t_2	6.8	0.8π	6.8
	$2a_1$	t_2	5.4	0.5π	4.1
		t_2	9.6	[c]	11.0
		t_2	18.5	[c]	20.8
$Sn(CH_3)_4$	$3t_2$	t_2	2.7	0.5π	4.0
		e	4.1		6.8
	$2a_1$	t_2	2.7	0.5π	4.0
		t_2	10.9	[c]	10.9
		t_2	20.4	[c]	20.4

[a] The resonance energy E_{phase} is given by the inflection point in the plot of the eigenphase sum vs photoelectron kinetic energy. [b] According to Kreile's[45] resonance criteria, the eigenphase sum must change by $\geq 0.3\pi$ over an energy range of $\Delta E \leq 6$ eV and $|E_{cross} - E_{phase}| \leq 4$ eV. [c] Change in eigenphase sum is continuous and $<0.3\pi$.

$(CH_3)_4$ no evidence of a t_2 resonance at ~20-eV kinetic energy was observed in either the $3t_2$ theoretical partial cross section or the experimental and theoretical branching ratios. A broad maximum does occur at ~43-eV kinetic energy in both the $3t_2$ theoretical partial cross section and branching ratio calculated for $Sn(CH_3)_4$. However, an examination of the eigenphase sum results indicated that this feature could not be considered a resonance. The minimum at ~40 eV in the $3t_2$ cross section of $Sn(CH_3)_4$ probably corresponds to the Sn 5p Cooper minimum. This feature is analogous to the I 5p Cooper minima in HI and CH_3I.[46] This minimum is not present in the $Si(CH_3)_4$ results because the Si 3p Cooper minimum is near threshold.

Between 30- and 50-eV photon energies, the $3t_2$ experimental branching ratios for $Si(CH_3)_4$ and $Sn(CH_3)_4$ are quite different. For $Sn(CH_3)_4$, the $3t_2$ branching ratio rises more steeply above 30 eV, reaching a maximum by ~40-eV photon energy. The Sn 4d ionization threshold occurs at ~31-eV photon energy. Like the I 4d and Xe 4d levels,[47,48] the Sn 4d cross section increases sharply to 40 eV and then to a maximum about 30 eV above threshold.[38] Since the $3t_2$ branching ratios of $Sn(CH_3)_4$ appear to mimic this behavior, Sn 5p → 4d interchannel coupling is probably important. A similar enhancement of 5p cross sections on scanning through the 4d levels has been observed in Xe and CF_3I.[19,49,50] Since interchannel coupling is not taken into account by the MS–Xα calculations, the experimentally determined branching ratios are in relatively poor agreement with the theoretical results in this region for $Sn(CH_3)_4$.

The results for the carbon–hydrogen bonding orbitals $1t_1 + 1e + 2t_2$, of $Si(CH_3)_4$ and $Sn(CH_3)_4$, are presented in Figure 4. These orbitals consist primarily of overlap of the C 2p orbitals (60%) with H 1s orbitals. The MS–Xα results indicate a smooth, rapid decline in both partial cross section and branching ratio with increasing photon energy after a broad maximum. The experimental branching ratios for both $Si(CH_3)_4$ and $Sn(CH_3)_4$ show a smooth decline in magnitude with increasing photon energy. The agreement between experimental and theoretical branching ratios is quite good at lower photon energies. These trends in partial cross section and branching ratio are typical for orbitals of considerable C 2p character.

In Figure 5 are given the results for the $2a_1$ molecular orbital of $Si(CH_3)_4$ and $Sn(CH_3)_4$. This is a metal–carbon bonding orbital containing primarily Si 3s (43%) or Sn 5s (56%) character as well as C 2p (36%) and H 1s contributions. The theoretical and experimental results for $Si(CH_3)_4$ and $Sn(CH_3)_4$ are remarkably similar, and theoretical and experimental branching ratios are in reasonable agreement. The $2a_1$ experimental branching ratios of $Sn(CH_3)_4$ follow the same trend as those for the better resolved $2a_1$ peak in the photoelectron spectra of $Si(CH_3)_4$. For each molecule, a distinct maximum in the $2a_1$ experimental branching ratio is observed at ~32-eV photon energy. The theoretical partial cross sections and branching ratios calculated for this orbital indicate the presence of a maximum at ~37-eV photon energy. The analysis of these results for the presence of shape resonances is simplified by the fact that all exit channels except t_2 are forbidden according to electric-dipolar-transition selection rules. The MS–Xα results indicated that a t_2 resonance is indeed present at 18.5-eV kinetic energy for $Si(CH_3)_4$ and 20.4-eV kinetic energy for $Sn(CH_3)_4$ (although this is probably not a shape resonance, Table IV). These resonance positions are at kinetic energy 2.0- and 4.4-eV higher than predicted experimentally for $Si(CH_3)_4$ and $Sn(CH_3)_4$, respectively. The greater discrepancy for the $Sn(CH_3)_4$ case is not particularly surprising, given the difficulty in fitting this peak from the photoelectron spectra. Nevertheless, the reasonable agreement between experimental and theoretical results provided confirmation of the location of this $2a_1$ orbital in $Sn(CH_3)_4$. The experimentally determined resonance position of 16.5-eV kinetic energy for $Si(CH_3)_4$ is in good agreement with the 18.0-eV term value of the t_2 resonance observed for $Si(CH_3)_4$ in the photoelectron and photoabsorption data above the Si 2p edge.[18,42]

Two other resonances at lower energy are predicted by the calculations (Figure 5, Table IV), but apart from a broadening of the $Si(CH_3)_4$ branching ratio, there is little evidence for these resonances. There is a hint of the Sn 5s Cooper minima at ~50 eV in the $Sn(CH_3)_4$ results.

The results for the $1a_1 + 1t_2$ molecular orbitals of $Si(CH_3)_4$ and $Sn(CH_3)_4$ are presented in Figure 6. These two orbitals, which are methyl carbon–hydrogen bonding orbitals, consist of overlap of the C 2s orbitals (~65%) with the H 1s orbitals. Some mixing of Si 3s (21%) or Sn 5s (10%) character into the $1a_1$ molecular orbital also occurs. The experimental branching ratios of these orbitals increase with increasing photon energy. Again, the $1a_1 + 1t_2$ branching ratios are very similar in magnitude for $Si(CH_3)_4$ and $Sn(CH_3)_4$. The theoretical branching ratios follow the trend of the experimental ones, although the magnitudes are in poor agreement, particularly at higher photon energies. The increase in branching ratio of these orbitals with photon energy is consistent with their considerable C 2s character. Since the intensity of the photoelectron band corresponding to ionization from the $1t_1 + 1e + 2t_2$ orbitals dominates the spectrum and the C 2p cross section falls off more rapidly than the C 2s cross section,[44] the $1a_1 + 1t_2$ branching ratios will increase with photon energy.

A similar valence-band cross section study of the analogues SF_6 and SeF_6[51] also shows that the experimental and theoretical results are very similar—as we have found here for $Si(CH_3)_4$ and $Sn(CH_3)_4$. Apparently, the cross sections are not very sensitive to the molecular potential—even for bonding orbitals. This conclusion is controversial but is unavoidable from these results.

Sn 4d Levels

The total Sn 4d cross section for $Sn(CH_3)_4$ determined from a transition-state MS–Xα calculation is displayed in the upper plot of Figure 7. The partial cross section curve generally increases from threshold to a broad maximum >30 eV above threshold. This behavior is qualitatively in agreement with the 4d partial cross sections of atomic tin measured previously.[38]

Good agreement is obtained between the experimental and theoretical Sn 4d branching ratios of $Sn(CH_3)_4$, which are illustrated in the lower plot of Figure 7. Much better agreement was obtained for a transition-state calculation than for the ground-state results used in the valence-band study. The branching ratio plots indicate a sharp rise in relative Sn 4d intensity above threshold that begins to level off above 55-eV photon energy.

(46) Carlson, T. A.; Fahlmen, A.; Krause, M. O.; Kelly, P. R.; Taylor, J. W.; Whitley, T.; Grimm, F. A. *J. Chem. Phys.* **1984**, *80*, 3521.
(47) Comes, F. J.; Nielsen, U.; Schwartz, W. H. E. *J. Chem. Phys.* **1973**, *58*, 2230.
(48) Shannon, S. P.; Codling, K.; West, J. B. *J. Phys. B* **1977**, *10*, 825.
(49) West, J. B.; Woodruff, P. K.; Codling, K.; Coulgate, R. G. *J. Phys. B* **1976**, *9*, 407.
(50) Krause, M. O. In *Synchrotron Radiation Research*; Winick, H., Doniach, S., Eds.; Plenum: New York, **1980**.
(51) Addison, B. M.; Tan, K. H.; Bancroft, G. M. *Chem. Phys. Lett.* **1986**, *129*, 468; submitted for publication in *J. Chem. Phys.*

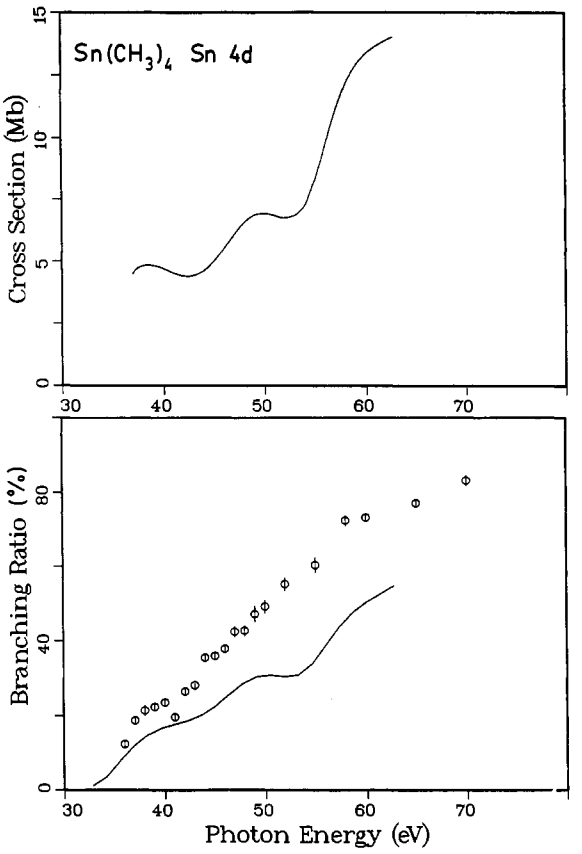

Figure 7. Experimental branching ratio and theoretical MS-Xα cross sections (σ) and branching ratios (solid lines) for the photoionization of the Sn 4d orbitals (total) of $Sn(CH_3)_4$.

The experimentally determined branching ratios of the spin–orbit components of the Sn 4d levels of $Sn(CH_3)_4$ are presented in the upper plot of Figure 8. The branching ratios of the $4d_{5/2}$ and $4d_{3/2}$ components show a trend similar to that of their total; both increase rapidly from 36.0 eV and level off toward higher photon energies. This dramatic increase in the intensity of the Sn 4d levels relative to the valence band, with increasing photon energy, parallels the results obtained previously for other organometallic tin compounds.[52]

The ratio of intensities of the spin–orbit components of the Sn 4d subshell of $Sn(CH_3)_4$ is illustrated in the lower plot of Figure 8. While the Sn 4d branching ratios could only be measured out to 70-eV photon energy because of the rapidly declining intensity of the valence band, the Sn 4d subshell branching ratio was readily measured to 100-eV photon energy. A spin–orbit splitting of 1.04 ± 0.03 eV was obtained from the spectra, in excellent agreement with that of other tin compounds.[52] With the use of a 50-eV electron analyzer pass energy, the spin–orbit components of the Sn 4d levels were not completely resolved and their line widths were constrained to be equal in fitting the spectra.

The Sn $4d_{5/2}$:$4d_{3/2}$ branching ratio deviates considerably from the statistical value of 1.5. At low photon energies, the branching ratio is larger than statistical and rapidly declines to a minimum of 1.55 ± 0.02 at 43.5-eV photon energy before rising to a maximum at 48.0-eV photon energy. The branching ratio passes through the statistical value of 1.5 at 56-eV photon energy and levels off to a relatively constant value of 1.42 ± 0.02 above 58-eV photon energy.

This trend in the Sn 4d subshell branching ratios is similar to that found in previous gas-phase experiments on the Xe 4d,[25] Cd 4d,[53] and Hg 5d[53,54] levels and in solid-state experiments on the

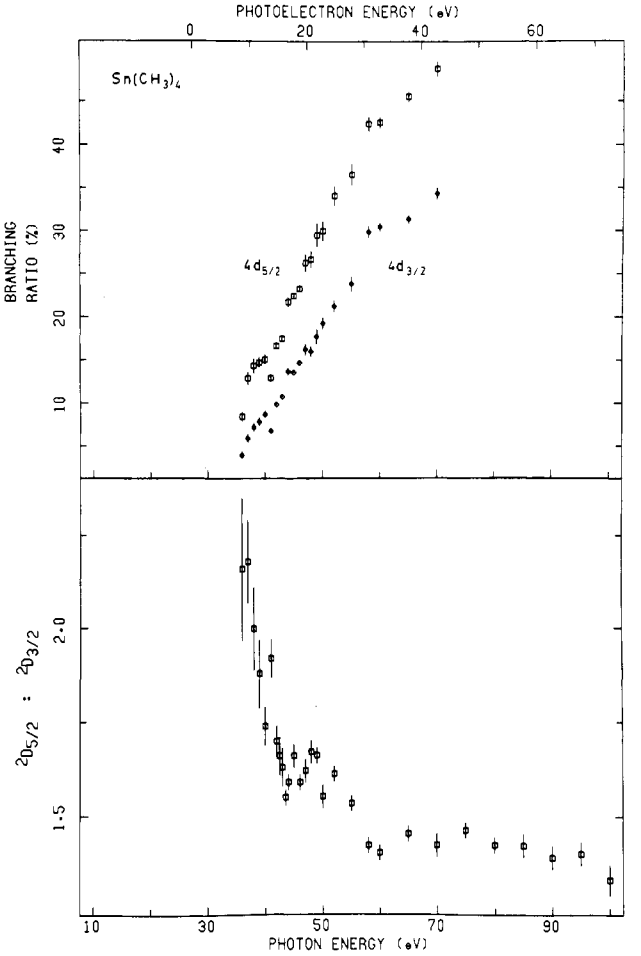

Figure 8. Experimental branching ratios for the spin–orbit components of the Sn 4d levels of $Sn(CH_3)_4$.

Pb 5d levels.[55] The substantial deviations of subshell branching ratios from their statistical values were described by Walker et al.[56,57] as being due to differing photoelectron kinetic energies for the two spin–orbit components and to differing radial wave functions of the two components. At low kinetic energies, the Sn 4d partial cross sections are increasing and the branching ratio is larger than statistical. The initial sharp decline in branching ratio is due to the onset of the $4d_{3/2}$ peak. At large photon energies where the kinetic energy effect is diminished, the partial cross sections are declining and the branching ratio will be more or less constant at a value below the statistical value. The maximum in the Sn 4d subshell branching ratio of $Sn(CH_3)_4$ presumably arises due to differences in the $4d_{5/2}$ and $4d_{3/2}$ partial cross sections per electron.

To assess the chemical dependence of this 4d branching ratio, we compare our results with the Sn 4d subshell branching ratios obtained from a study of solid-state SnS_2.[58] The trend in Sn 4d branching ratios observed for $Sn(CH_3)_4$ is very similar to that obtained for SnS_2. For solid SnS_2, the minimum in Sn 4d subshell branching ratio occurred at ~39-eV photon energy while the maximum occurred at ~43-eV photon energy. The shift of these positions to 5 eV lower energy relative to the corresponding values for gaseous $Sn(CH_3)_4$ can be explained by the work function of the solid sample ($E_{vacuum} - E_{Fermi}$). However, the Sn 4d intensity

(52) Bancroft, G. M.; Sham, T. K.; Eastman, D. E.; Gudat, W. *J. Am. Chem. Soc.* **1977**, *79*, 1752.
(53) Johnson, W. R.; Radojevic, V.; Deshmukh, P.; Cheng, K. T. *Phys. Rev. A* **1982**, *25*, 337 and references therein.
(54) Kobrin, P. H.; Heimann, P. A.; Kerkhoff, H. G.; Lindle, D. W.; Truesdale, C. M.; Ferrett, T. A.; Becker, U.; Shirley, D. A. *Phys. Rev. A* **1983**, *27*, 3031.
(55) Bancroft, G. M.; Gudat, W.; Eastman, D. E. *Phys. Rev. B* **1978**, *17*, 4499.
(56) Walker, T. E. H.; Berkowitz, J.; Dehmer, J. L.; Waber, J. T. *Phys. Rev. Lett.* **1975**, *31*, 678.
(57) Walker, T. E. H.; Waber, J. T. *J. Phys. B* **1974**, *7*, 674.
(58) Margaritondo, G.; Rowe, J. E.; Christman, S. B. *Phys. Rev. B: Condens. Matter* **1979**, *19*, 2850.

ratio of SnS_2 appeared to pass through the statistical value of 1.5 at ~45 eV, a shift of 11 eV to lower photon energy from that of $Sn(CH_3)_4$. This distinct difference suggests that the partial cross section behaviors of the Sn $4d_{5/2}$ and $4d_{3/2}$ components differ between $Sn(CH_3)_4$ and SnS_2. While solid-state effects may play some role in these differences, their contribution is considered to be minor.[58] Therefore, chemical environment does appear to influence the $4d_{5/2}$ and $4d_{3/2}$ cross sections, as previously noted for Hg in Hg atoms and Me_2Hg.[21]

Conclusions

Experimental branching ratios have been determined for the valence levels of $Si(CH_3)_4$ and the valence and Sn 4d levels of $Sn(CH_3)_4$ as a function of photon energy. A comparison of the experimental results with theoretical results obtained from nonrelativistic MS-Xα calculations on $Si(CH_3)_4$ and $Sn(CH_3)_4$ indicate reasonably good agreement. This agreement confirms the assignment of the valence-band spectrum as $3t_2 < 1t_1 \sim 1e \sim 2t_2 < 2a_1 < 1t_2 \sim 1a_1$, in order of increasing binding energy. This is also the ordering predicted from the MS-Xα calculation on $Si(CH_3)_4$. The earlier assignment based on CNDO/2 calculations[4] on $Si(CH_3)_4$, $3t_2 < 1t_1 < 2a_1 < 1e < 2t_2 < 1t_2 < 1a_1$, can be considered incorrect for determining the $2a_1$ orbital binding energy.

When the Sn 4d levels of $Sn(CH_3)_4$ are excluded, the valence band branching ratios of $Sn(CH_3)_4$ and $Si(CH_3)_4$ are extremely similar and are dominated by the rapid decline in intensity of the $1t_1 + 1e + 2t_2$ molecular orbitals with increasing photon energies. As a result, the $3t_2$ and $2a_1$ metal–carbon bonding orbitals appear to increase in intensity with increasing photon energy, since their partial cross sections are declining at a slower rate.

Intershell correlation between the Sn 5p electron contribution (30%) to the $3t_2$ orbital and the Sn 4d shell appears to be present in the experimental $3t_2$ branching ratios of $Sn(CH_3)_4$. However, no evidence of Sn 5s → 4d interchannel coupling is apparent in the $2a_1$ experimental branching ratios even though the $2a_1$ orbital contains ~56% Sn 5s character. By comparison, Hg 6s → 5d interchannel coupling is present in the $3a_1'$ experimental branching ratios of $Hg(CH_3)_2$.[21] This orbital contains ~60% Hg 6s character. In a similar study of the 4e and $4a_1$ branching ratios of CF_3I, strong intershell correlation was found between the I 4d shell and the 4e orbital but not the $4a_1$ orbital even though both contain substantial I 5p character.[19] This was rationalized by considering intershell correlation effects to be largest when localized core electrons are interacting with valence-orbital electrons localized on the same atom. In keeping with this interpretation, the $3t_2$ orbital of $Sn(CH_3)_4$ and the $3a_1'$ orbital of $Hg(CH_3)_2$ are localized on the metal center while the $2a_1$ orbital of $Sn(CH_3)_4$ is more delocalized.

This branching ratio behavior of the valence orbitals of $Si(CH_3)_4$ and $Sn(CH_3)_4$ may be rationalized without the direct inclusion of Si 3d or Sn 5d orbital character. However, the possible involvement of these orbitals in bonding cannot be strictly ruled out by this present study. The t_2 shape resonance observed at 18.0 eV above the Si 2p edge in photoionization and electron-impact measurements on $Si(CH_3)_4$ has been observed in the branching ratio behavior of the $2a_1$ molecular orbital. A similar resonance appears in the experimental and theoretical results for the $2a_1$ orbital of $Sn(CH_3)_4$. Predicted lower energy resonances need to be examined by using photon energies between 10 and 20 eV.

Overall, the cross section and resonance behavior of $Si(CH_3)_4$ is very similar to that of $Sn(CH_3)_4$. This parallels the similarities in resonance behaviors of SF_6 and SeF_6.[51] These results are in sharp contrast to the radically different cross section and resonance behavior observed for CF_4 and SiF_4. It appears that, beyond the first-row elements, the nature and geometry of the ligands are primarily responsible for the observed resonance behavior rather than the details of the molecular potential. Recent theoretical MS-Xα calculations showed that cross section features at high kinetic energy (>20 eV) are primarily due to electron diffraction from the ligands.[51] The results for $Ge(CH_3)_4$[59] will be interesting now to confirm our hypothesis.

The $4d_{5/2}$:$4d_{3/2}$ branching ratio for $Sn(CH_3)_4$ was found to differ significantly from that for SnS_2. The minimum and maximum in the branching ratio curve were shifted to 5 eV lower energy due to the work function of solid-state SnS_2. The shift of the statistical crossing point to 11 eV lower energy in SnS_2 signifies a difference in chemical environment. Considering the solid-state effects to be minimal and the Sn 4d levels to not be involved in bonding, chemical environment appears to directly affect the subshell branching ratio, probably by affecting the outgoing f wave potential.

Acknowledgment. We acknowledge the assistance of the staff at the Synchrotron Radiation Center (Stoughton, WI) and the technical assistance of L. L. Coatsworth. We are grateful to the National Research Council of Canada (NRC), the Natural Sciences and Engineering Research Council of Canada (NSERC), and The University of Western Ontario for financial support.

Registry No. $Si(CH_3)_4$, 75-76-3; $Sn(CH_3)_4$, 594-27-4; Sn, 7440-31-5.

(59) Cavell, R. G.; personal communication.